Smooth Seamless Surface Construction Based on Conformal Self-organizing Map

Cheng-Yuan Liou, Yen-Ting Kuo, and Jau-Chi Huang

Department of Computer Science and Information Engineering
National Taiwan University
cyliou@csie.ntu.edu.tw
Supported by NSC 94-2213-E-002-034

Abstract. This paper presents a method to construct a smooth seamless conformal surface for the genus-0 manifold. The method is developed for the conformal self-organizing map [10]. The constructed surface is both piecewise smooth and continuous. The mapping between the model surface and the sphere surface is one-to-one and onto. We show experiments in surface reconstruction and texture mapping.

1 Introduction

The goal of surface reconstruction is to obtain a continuous surface that can represent a cloud of pattern points [2]. These cloud patterns are usually obtained from 3D laser scanners and medical scanners. These patterns may also be collected by various vision techniques, such as correlated viewpoints, voxel carving, stereo range images. Let X denote the set that contains all point patterns, $X = \{(x_l, y_l, z_l)^T, l = 1, .., P\}$. The conformal self-organizing map (CSM) [9][10] derives a continuous surface for the cloud patterns using a collection of connected simplices including points, edges, and triangles. It is a kind of self-organizing map [7] with conformal contents [8]. Since these triangles are flat, the surface constructed by these flat triangles is a continuous surface but not a smoothly curved one. Besides, the flat triangle surface in 3D [10] has ambiguous mapping correspondence on the triangle edges. In this paper we show how to construct a piecewise smooth seamless surface with unique correspondence based on the derived surface by the CSM.

Basic terminology
Let the collection of all triangles inside a unit sphere be $S^{\Delta} = \{\Delta_n^r, r = 1, ..., R\}$ as illustrated in Fig. 1(b). Let the collection of all vertices (nodes) be $\mathbb{N} = \{n_i, i = 1, ..., N\}$, where n_i is a 3D column vector in the network space and contains the position of the i^{th} mesh vertex on the unit sphere surface. Each triangle is a mesh hole that can be represented by its three vertices, that is, $\Delta_n^r \equiv [n_i^r, n_j^r, n_k^r]$. The mesh of S^{Δ} can be generated by geodesic dome [6].

Review the CSM
In the CSM, the sampled 3D patterns are the training patterns and the mesh is configured by neurons. These neurons are the vertices of the mesh. Each neuron

I. King et al. (Eds.): ICONIP 2006, Part I, LNCS 4232, pp. 1012–1021, 2006.
© Springer-Verlag Berlin Heidelberg 2006

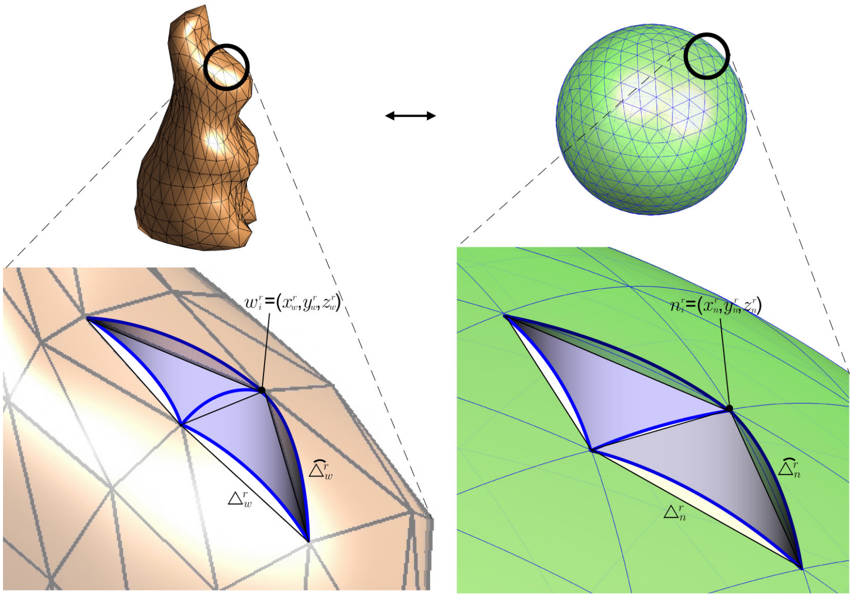

(a) data pattern space (b) network space

Fig. 1. Illustration of the pattern space X and the network space in the CSM. (a) The model surface. (b) The neurons' position vectors. The curved domes are shown with blue arcs.

has two vectors, one is the weight vector, w_i, in the pattern space and the other is the position vector, n_i, in the network space. The weight vectors contain the locations of the mesh vertices in the pattern space. The position vectors contain the locations of the neurons on the sphere surface. Fig. 1 shows the relationship of these two vectors. In the CSM, w_i is evolved to match its corresponding pattern and n_i is fixed to preserve the sphere topology.

The CSM constructs a mapping from S^{Δ} to M^{Δ} [10], where M^{Δ} is the manifold of the sample points. M^{Δ} is the constructed model surface or the manifold surface to represent the cloud X. M^{Δ} is the surface formed by a collection of the flat triangles, $M^{\Delta} = \{\Delta_w^r, r = 1, ..., R\}$. By using the CSM, each equilateral triangle Δ_n^r is mapped to its corresponding triangle Δ_w^r. Δ_w^r is an irregular triangle and a mesh hole that can be represented by its three vertices, that is, $\Delta_w^r = [w_i^r, w_j^r, w_k^r]$, where w_i^r is a 3D column weight vector in the pattern space and contains the position of the i^{th} mesh vertex in M^{Δ}, see Fig. 1(a). The vertex w_i^r is mapped to the vertex n_i^r. Both Δ_w^r and Δ_n^r are flat triangles. In the CSM, the parameterization domain is the surface S^{Δ} which is suitable for the genus zero manifold. The set $\mathbb{N}$ contains all joint points shared by S^{Δ} and the unit sphere surface, S.

There are ways to construct a smooth dome over the Δ_w^r, such as fitting a triangular surface spline[3][4]. Since the sphere surface is both continuous and smooth, these fine properties are useful in building other surface. We show how to map (borrow) the sphere surface, S, to its corresponding model surface based on the derived M^{Δ}. The detailed method is in the next section. Results are given in the Section 3.

2 Smooth Seamless Surface Parameterization

By using the CSM [10], we can derive the M^{Δ} and obtain the mapping between each triangle Δ_n^r and its corresponding triangle Δ_w^r. Let the portion of the sphere surface right above the flat triangle, Δ_n^r, be $\widehat{\Delta_n^r}$, see Fig. 1(b). The triangular dome $\widehat{\Delta_n^r}$ can be obtained by cutting the three arc curves, $\{\widehat{n_i^r n_j^r}, \widehat{n_j^r n_k^r}, \widehat{n_i^r n_k^r}\}$, on the sphere surface right above the three edges, $\{\overline{n_i^r n_j^r}, \overline{n_j^r n_k^r}, \overline{n_i^r n_k^r}\}$, of the triangle Δ_n^r. Each arc point is the intersection of the sphere surface and the line that passes through the sphere center, $c = (0,0,0)^T$, and an edge point. The arc $\widehat{n_i^r n_j^r}$, edge $\overline{n_i^r n_j^r}$, and center c are in the same plane. $\widehat{\Delta_n^r}$ is the geodesic dome of Δ_n^r and has a triangular tent shape. The sphere surface, S, is the collection of every $\widehat{\Delta_n^r}$, $S = \{\widehat{\Delta_n^r}, r = 1, ..., R\}$. Since the dome $\widehat{\Delta_n^r}$ is beautiful that is both smooth and continuous, we want to borrow and fit (deform) the dome to construct a smooth model surface for the cloud X. In the following algorithm, we show how to map each $\widehat{\Delta_n^r}$ to its corresponding dome, $\widehat{\Delta_w^r}$, to obtain a smooth model surface, M, where $M = \{\widehat{\Delta_w^r}, r = 1, ..., R\}$.

The algorithm to accomplish the $\widehat{\Delta_w^r}$ is in below.

Smooth Algorithm

Input: new dense mesh $\mathbb{N}^{new}$, sphere mesh S^{Δ}, model mesh M^{Δ}.
Output: smooth surface M.

1. For each triangle Δ_n^r, $\Delta_n^r \in S^{\Delta}$, find the center c_n^r of the triangle Δ_n^r and its conformal mapping point, c_w^r, in Δ_w^r, see Fig. 2.
2. Separate Δ_w^r, $\Delta_w^r \in M^{\Delta}$, into three subtriangles, $\{[c_w^r, w_i^r, w_j^r], [c_w^r, w_j^r, w_k^r], [c_w^r, w_i^r, w_k^r]\}$, by using the three line sections, $\{\overline{c_w^r w_i^r}, \overline{c_w^r w_j^r}, \overline{c_w^r w_k^r}\}$, and the three edges, $\{\overline{w_i^r w_j^r}, \overline{w_j^r w_k^r}, \overline{w_i^r w_k^r}\}$.
3. Calculate the unit normal vector of the triangle plane Δ_w^r (Fig. 3):
$$\widehat{n}_w^r = \frac{\left(w_j^r - w_i^r\right) \times \left(w_k^r - w_i^r\right)}{\left|\left(w_j^r - w_i^r\right) \times \left(w_k^r - w_i^r\right)\right|}. \tag{1}$$
4. Let the triangle next to Δ_w^r in M^{Δ} that shares the edge $\overline{w_i^r w_j^r}$ is $\Delta_w^{r^1}$, that shares the edge $\overline{w_j^r w_k^r}$ is $\Delta_w^{r^2}$, that shares the edge $\overline{w_i^r w_k^r}$ is $\Delta_w^{r^3}$. Calculate the unit normal vectors of the three adjacent triangles, $\Delta_w^{r^1}$, $\Delta_w^{r^2}$, $\Delta_w^{r^3}$, by using the same equation in the above step. Let the obtained normal vectors be $\widehat{n}_w^{r^1}$, $\widehat{n}_w^{r^2}$, and $\widehat{n}_w^{r^3}$ respectively (Fig. 3).

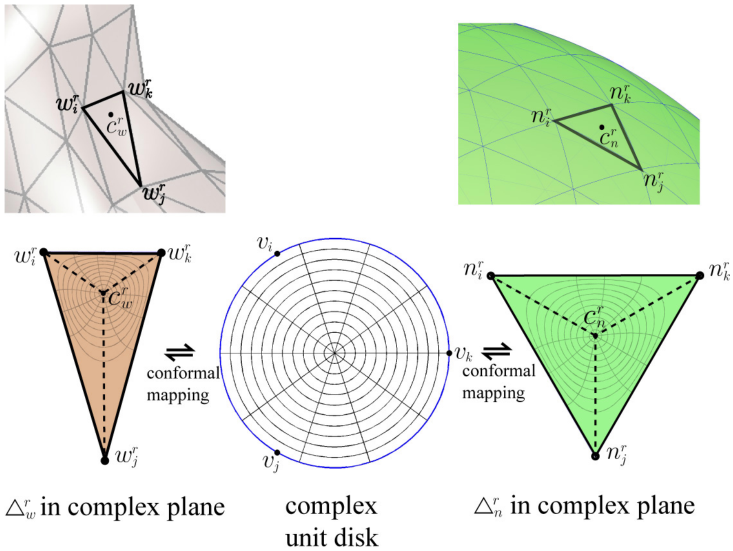

Fig. 2. onformal mapping between the two triangles Δ_n^r and Δ_w^r. Each traingle in 3D is translated to the complex plane. Then their conformal mappings to a unit disk can be computed by the Schwarz–Christoffel method [11] to build the point correspondence.

5. Calculate the unit normal vectors of the edges, $\overline{w_i^r w_j^r}$, $\overline{w_j^r w_k^r}$, and $\overline{w_i^r w_k^r}$:

$$\widehat{e}_w^{r^1} = \frac{\widehat{n}_w^r + \widehat{n}_w^{r^1}}{\left|\widehat{n}_w^r + \widehat{n}_w^{r^1}\right|},\ \widehat{e}_w^{r^2} = \frac{\widehat{n}_w^r + \widehat{n}_w^{r^2}}{\left|\widehat{n}_w^r + \widehat{n}_w^{r^2}\right|},\ \text{and}\ \widehat{e}_w^{r^3} = \frac{\widehat{n}_w^r + \widehat{n}_w^{r^3}}{\left|\widehat{n}_w^r + \widehat{n}_w^{r^3}\right|}. \tag{2}$$

Note that $\widehat{e}_w^{r^1} \perp \overline{w_i^r w_j^r}$, $\widehat{e}_w^{r^2} \perp \overline{w_j^r w_k^r}$, and $\widehat{e}_w^{r^3} \perp \overline{w_i^r w_k^r}$ (Fig. 3).

6. Select a point p on $\widehat{\Delta_n^r}$, $p \in \mathbb{N}^{new}$. Find its projection, p', on the flat triangle Δ_n^r:

$$p' \equiv \overline{pc} \cap \Delta_n^r. \tag{3}$$

Here $c = (0,0,0)^T$ is the center of the unit sphere and p' is the intersection point of the line $\overline{pc}$ and Δ_n^r, as shown in Fig. 4(a).

7. For the point p', calculate its conformal mapping point q' in Δ_w^r,

$$q' = \mathcal{M}_{\Delta_n^r}^{\Delta_w^r}(p'), \tag{4}$$

where $\mathcal{M}_{\Delta_n^r}^{\Delta_w^r}$ is the conformal mapping [10] from the flat triangle Δ_n^r to the flat triangle Δ_w^r, see Fig. 4(b). q' may fall in any one of the three subtriangles. Suppose q' is in the subtriangle $[c_w^r, w_i^r, w_j^r]$.

8. Calculate the projection point $b_{q'}$ of q' on the line section $\overline{w_i^r w_j^r}$. This means that $\overline{w_i^r w_j^r} \perp \overline{b_{q'} q'}$. Calculate the intersection point $a_{q'}$ of the line $\overline{b_{q'} q'}$ and one of the other two edges of the subtriangle $[c_w^r, w_i^r, w_j^r]$. The locations of $a_{q'}$ and $b_{q'}$ are shown in Fig. 3.

9. Calculate the unit direction $\widehat{n}_{q'}$ at the point q' :

$$\widehat{n}_{q'} = \frac{\overrightarrow{n}_{q'}}{|\overrightarrow{n}_{q'}|},$$
$$\overrightarrow{n}_{q'} = \frac{|q' - a_{q'}|}{|b_{q'} - a_{q'}|} \left(\widehat{e}_w^{r^1} - \widehat{n}_w^r \right) + \widehat{n}_w^r. \tag{5}$$

   Note that q', $a_{q'}$, $b_{q'}$, and $\widehat{n}_{q'}$ are in the same plane. The two vectors $\widehat{e}_w^{r^1}$ and $\widehat{n}_w^r$ in Fig. 3 which pass the points $b_{q'}$ and $a_{q'}$ separately are also in this plane.

10. In this step we plan to determine a point $q \in M$, for the dome $\widehat{\Delta_w^r}$ that is correspond to p. q is obtained from the dome height $|p - p'|$ and the unit direction $\widehat{n}_{q'}$. q can be obtained by

$$q = q' + |p - p'| \, \widehat{n}_{q'}. \tag{6}$$

   The whole construction is shown in Figs. 4 and 3.

11. Repeat step 6 and select another point, $p \in \mathbb{N}^{new}$, iteratively.

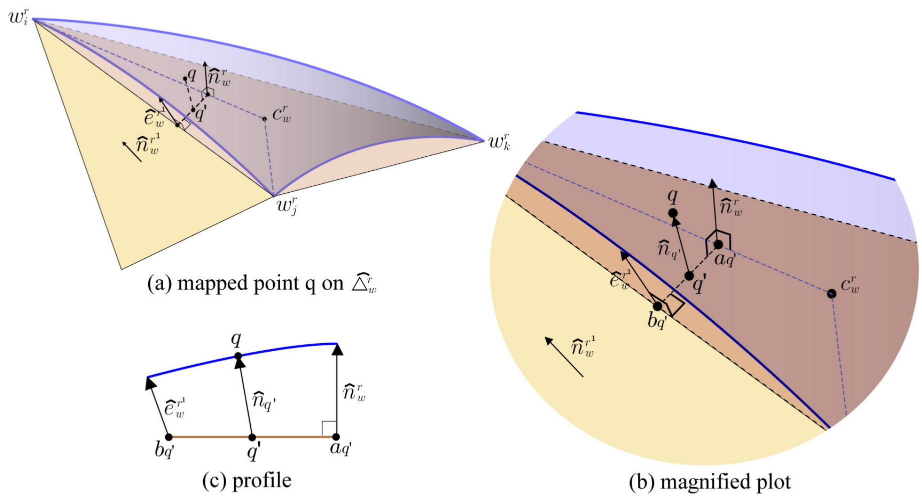

Fig. 3. Illustration of the relations between the points p and q

We operate this algorithm on all R triangles. We may map any number of surface points for each triangle dome. This mapping is bijection which maps from the triangular sphere surface $\widehat{\Delta_n^r}$ to the triangular geodesic model surface $\widehat{\Delta_w^r}$. The surface border of $\widehat{\Delta_w^r}$ along the three boundary arc curves, $\{\widehat{w_i^r w_j^r}, \widehat{w_j^r w_k^r}, \widehat{w_i^r w_k^r}\}$, is perfectly seamless and continuous but may not be smooth. To our knowledge, this is the only seamless arc connecting two triangular domes.

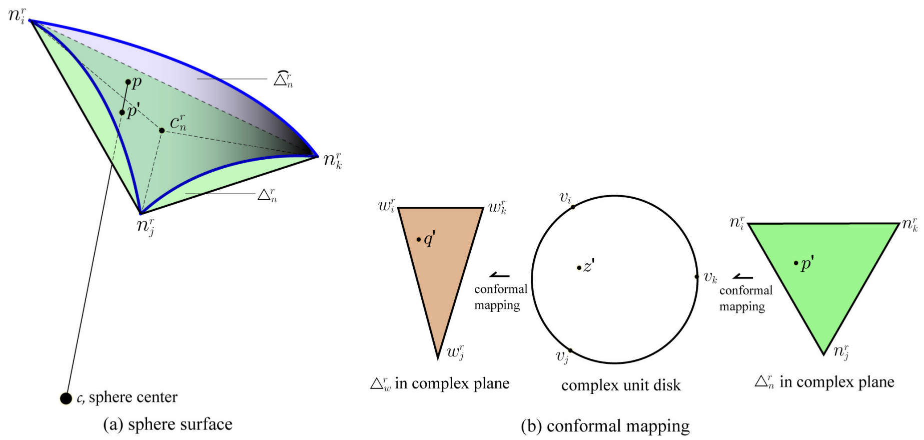

Fig. 4. Illustration of the relations among the points p, p', q' and c

In all experiments, the surface point p on $\widehat{\Delta_n^r}$ is a vertex of a new denser mesh $\mathbb{N}^{new}$, where $N^{new} > N$. $\mathbb{N}^{new}$ may be an icosahedron with more vertices. $\mathbb{N}^{new}$ may have dense vertices in an area with fine texture.

We assert, without proof, that the mapping of each $\widehat{\Delta_n^r}$ to its corresponding dome, $\widehat{\Delta_w^r}$, is bijection, Lemma 1. $f_p : p \to p'$ is bijective; Lemma 2. $\mathcal{M}_{\Delta_n^r}^{\Delta_w^r} : p' \to q'$ is bijective; Lemma 3. $f_q : q' \to q$ is bijective. This mapping is from the triangular sphere surface Δ_n^r to the triangular geodesic model surface Δ_w^r. We also assert, without proof, that the mapping of each subtriangular dome $\widehat{\Delta_n^{r^i}}$ to its corresponding dome, $\widehat{\Delta_w^{r^i}}$, is smooth.

3 Implementation and Results

The goal of this smooth seamless surface (SSS) construction is to accomplish a surface of a real object than a triangular mesh. To verify it, we prepare two sets of sampled points of a same object. One has fewer points, denoted as X_{few}, and the other has more points, denoted as X_{more}. Let CSM compute the conformal mapping using the fewer one. We then apply SSS to improve it and obtain the model surface M. The performance is evaluated by the mean square error. The error is named as mismatch error, E_{mis}. It is

$$E_{mis} = \frac{1}{\#\left(X_{more}\right)} \sum_{x \in X_{more}} dist\left(x, M\right)^2 . \tag{7}$$

The distance from point x to surface M, $dist\left(x, M\right)$, is the projection distance from x to M.

In certain case, such as the bunny model has long extrude parts, the ears, it is difficult for the CSM to learn those concave ear shapes. An edge swap with multi-resolution learning [12] and a growing neural mesh [5] may be used to overcome this difficulty. However, since they change the regular mesh connection, we will not use them in the CSM. We solve this difficult learning by giving the priority to those extrude parts during the CSM learning. This priority can resolve those parts and keep the regular connection.

There are two models used in experiments including the Stanford bunny [14] and the Igea head [13]. The mesh size of these models is listed in Table 1 below.

Table 1. Model parameters

	Igea model		bunny model	
	vertices	faces	vertices	faces
X_{few}	12,963	25,922	12,963	25,921
X_{more}	134,345	268,686	35,947	69,451
CSM	12,962	25,920	12,962	25,920
dense mesh $\mathbb{N}^{new}$	64,002	128,000	64,002	128,000

In the CSM learning phase, we set the number of training epoch be $epoch =$ 80.In each epoch, 8000 random sample patterns are used in the learning. The parameters for the neighborhood variance are set as $\sigma_0 = 0.4$ and $\tau_1 = 20$. The parameters for the learning rate are set as $\alpha_0 \leftarrow 0.01$ and $\tau_2 \leftarrow 60$. The training parameters *epoch*, σ_0, τ_1, α_0, and τ_2 are defined in [10]. The mismatch error E_{mis} of SSS is listed in Table 2. The SSS results are shown in Fig. 5.

Table 2. Mismatch error

Igea model		bunny model	
	E_{mis}		E_{mis}
SSS	1.4169×10^{-5}	SSS	5.2631×10^{-5}
mesh of X_{few}	8.0370×10^{-5}	mesh of X_{few}	1.0890×10^{-4}

One of the reason for building the smooth surface is to facilitate the texture mapping. So, one can trace the texture details equally on the smooth surface without any ambiguous correspondence. The texture mapping of a genus zero manifold is achieved in the following way. Suppose there are a texture image I, model surface M, and sphere surface S. First we select a desired view point of the model M and the north pole of sphere S based on the view point. Then apply stereographic projection from image I to sphere S. Then map the image I from the sphere S to the model surface M. We use this projection is because it is a conformal mapping and is very regular near the point of tangency. Fig. 6(a) shows the result of a crocodile skin texture mapped on the bunny model. In Fig. 6(b), the checkerboard texture is mapped on the surface. A facial makeup of Chinese operas in Fig. 6(c) is mapped to the smooth surface in Fig. 6(d).

Fig. 7 shows two texture mapping cases. Fig. 7(a,b) show the checkerboard texture on the smooth Igea surface in Fig. 5(c). A facial makeup in Chinese opera in Fig. 7(c) is mapped on the smooth Igea surface, see Fig. 7(d).

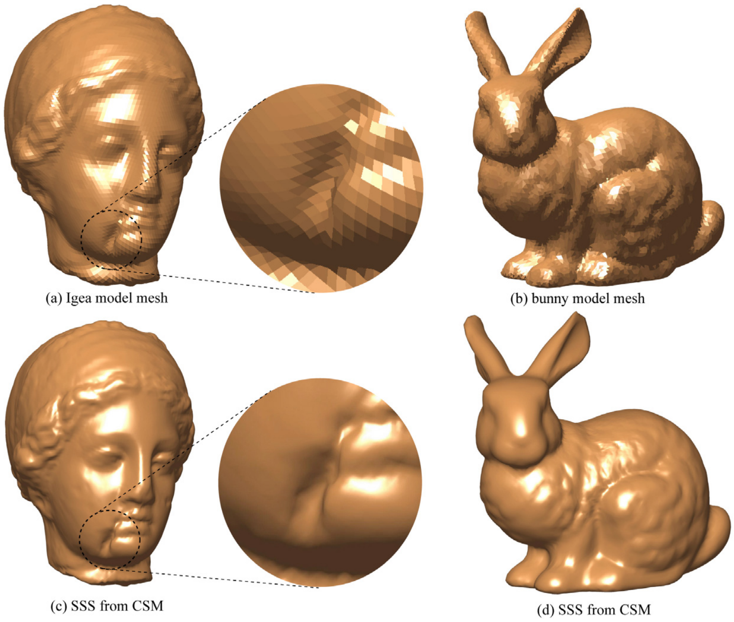

Fig. 5. (a-b) The original model mesh (c-d) The SSS surface from CSM

Fig. 6. (a) The model surface M by the smooth algorithm. (b) The checkerboard texture mapping on M. (c) The 2D facial makeup in Chinese opera. (d) The facial texture mapping on M.

Fig. 7. Texture mapping on the Igea's head. (a,b) The checkerboard texture mapping. (c) The 2D facial makup in Chinese opera. (d) The facial makeup mapping on the Igea's head.

4 Discussion

The smooth algorithm accomplishes the curved smooth surface instead of the flat triangle surface obtained from the CSM. The CSM by Liou and Tai in [7] was designed, originally, to trace the system state which changes continuously and to resolve various severe competitions among finite neurons in the self-organizing map (SOM). The SOM with finite neurons cannot be used for monitoring the continuous state. The folded mapping in SOM can be indicated and resolved by the negative values of the Jacobian of the mapping function [8]. The CSM can save and accommodate fine textures in the map. The CSM with flat triangle surface in 3D [10] has ambiguous resolution on the triangle edges. So, the 3D surfaces S^{Δ} and M^{Δ} are not suitable for tracing the continuous state. The surfaces S and M will do. Note that the CSM [7] in 2D flat plane does not have such ambiguous problem.

Instead of a surface with flat triangles, a curved smooth parameterization for unorganized data patterns is accomplished for the model surface. This smooth surface serves as a kind of interpolation for the CSM mesh. Since the sphere surface possesses well behaved smooth properties, we expect the SSS can carry the full extent of these beautiful properties to the model surface.

Texture mapping is a direct application of the SSS. The proposed algorithm can be additively applied to many triangular meshes obtained by existing methods. Potential applications are the brain-to-brain registration, consistent parameterization [1], facial expression synthesis, deformable object simulation and computing geodesic path on a model surface. The parameterization for higher genus is also under our study.

References

1. Asirvatham, A., Praun, E., Hoppe, H.: Consistent spherical parameterization. In International Conference on Computational Science, Singapore (2005) 265-272
2. Dinh, H.Q., Turk, G.: A sampling of surface reconstruction techniques. Research Report, Graphics, Visualization, and Usability Center, Georgia Institute of Technology (2000) GVU-00-28.
3. Hoffmann, M.: Local update of B-spline surfaces by Kohonen neural network. In Proceedings of the 5th International Conference on Computer Graphics and Artificial Intelligence, Limoges (2002) 103-112
4. Hoppe, H., DeRose, T., Duchamp, T., Halstead, M., Jin, H., McDonald, J., Schweitzer, J., Stuetzle, W.: Piecewise smooth surface reconstruction. Computer Graphics **28** (1994) 295-302
5. Ivrissimtzis, I.P., Jeong, W.K., Lee, S., Lee, Y., Seidel, H.P.: Neural meshes: surface reconstruction with a learning algorithm. Research Report, Max-Planck-Institut Informatik (2004) MPI-I-2004-4-005.
6. Kenner, H.: Geodesic math and how to use it. University of California Press, Berkeley (1976)
7. Liou, C.-Y., Tai, W.-P.: Conformal self-organization for continuity on a feature map. Neural Networks **12** (1999) 893-905
8. Liou, C.-Y., Tai, W.-P.: Conformality in the self-organization network. Artificial Intelligence **116** (2000) 265-286
9. Tai, W.-P., Liou, C.-Y.: Image representation by self-organizing conformal network. The Visual Computer **16(2)** (2000) 91-105
10. Liou, C.-Y., Kuo, Y.-T.: Conformal self-organizing map for a genus-zero manifold. The Visual Computer **21(5)** (2005) 340-353
11. Nehari, Z.: Conformal Mapping, McGraw-Hill, New York (1952)
12. Yu, Y.: Surface reconstruction from unorganized points using self-organizing neural networks. In IEEE Visualization 99, Conference Proceedings, San Francisco, California (1999) 61-64
13. Cyberware designs, manufactures, and sells standard and custom 3D scanning systems and software (2005), http://www.cyberware.com/samples/
14. Stanford Computer Graphics Laboratory, Data archives (2004) http://www-graphics.stanford.edu/data/